Pressure Distribution on the Surface near the Cylinder–Body Juncture

by

Fumio Yoshino* and Ryoji Waka*

This investigation is concerned with the static-pressure distributions on two surfaces, i. e., those of a side-wall and a circular cylinder with blowing. It was found that the results of this investigation were quite consistent with the flow pattern established by a series of investigations conducted in our laboratory.

1 Introduction

It has been well known that the complex flow pattern near the high-lifting-surface-body juncture becomes further complex because of the secondary flow. And it is extremely difficult to analyse that flow quantitatively. Then an attempt was made to visualize the flow around a circular cylinder with blowing by means of several techniques, that is, the dye-injection method, the tuft method and the oil-flow method. In a series of these investigations[1,2,3] and others,[4,5,6] the flow pattern near the juncture has been mostly established.

In this report we describe the pressure distributions on the side-wall and the cylinder with and without blowing in order to further confirm those results of investigations.

2 Nomenclatures

C_{lc} = Sectional lift coefficient at the mid-span ;
C_p = Static-pressure coefficient ;
C_μ = Momentum coefficient of the jet ;
D = Diameter of the cylinder ;
R_e = Reynolds number based on D and U_∞ ;
U_∞ = Main flow speed ;

* Department of Mechanical Engineering

x, y and z = Distances from the mid-span in streamwise, spanwise and upward
                directions, respectively ;

y_w = Distance from the side-wall in spanwise direction ;

θ_j = Angular position of the blowing slot.

3   Experimental installment and method

The apparatus for this experiment was the same one described in the references
2) and 4), and is not repeated here in detail.

The cross section of the circular cylinder and the assembly drawing of the model
are shown in Figs. 1 and 2, respectively. The model consists of two partition-plates
called the side-wall from now on and a cylinder with a blowing slot, 0.59 mm width,
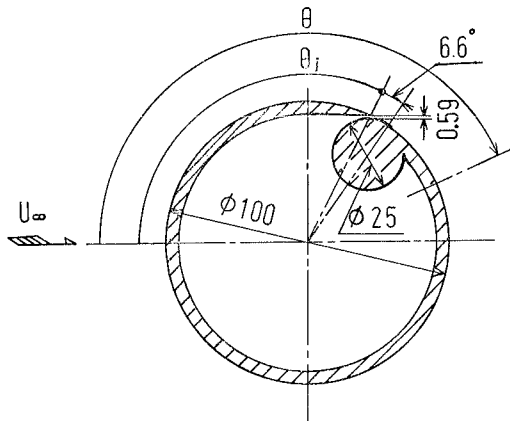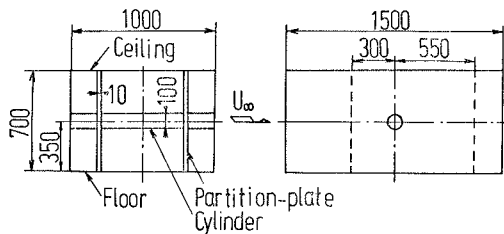along the whole span.

The arrangements of 166 static-pressure
holes on the starboard side-wall and 335
static-pressure holes on the cylinder are
shown in Fig. 3 and Table I, respectively.
The experiment was made by properly
varying C_μ and θ_j at the fixed values of
the aspect ratio of eight and the Reynolds
numbers of 1.5×10^5 and 2.1×10^5. The
ranges of C_μ and θ_j were from 0 to 0.37
and from 50° to 120°, respectively.

Fig. 1 Cross section of the cylinder.
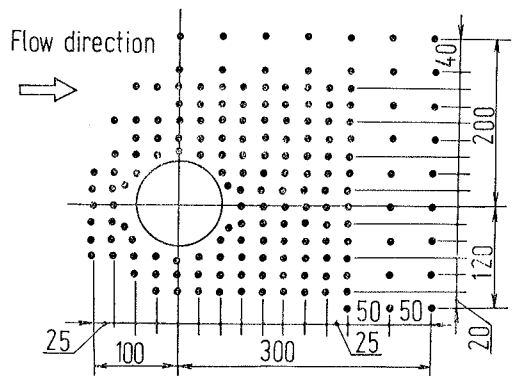
Fig. 2 Assembly drawing of the model.

Fig. 3 Arrangement of the static-pressure
holes on the side-wall.

Table I   Arrangement of the static-pressure
holes on the cylinder.

Row	y_w(mm)	Angular position	Total
1	3.0	At intervals of 10° from the first hole* to the 24th and of 15° from the 24th to the 31st .	155
3	20.3		
4	40.3		
6	73.0		
7	91.0		
2	10.3	At intervals of 10° from the first hole* to the 28th and of 15° from the 28th to the 31st .	124
5	55.3		
8	111.0		
9	164.0		
10	400.0	At intervals of 6° from the first hole* to the 56th .	56

* There is the first static-pressure hole
at $\theta = \theta_j + 6.6°$.

4   Results and Discussion

The pressure on the side-wall when $C_\mu = 0$ and $C_\mu = 0.25$ are shown in Figs. 4
and 5, respectively. The circles in these figures indicate the positions at which
they take the values assigned to in the figures. Those positions were obtained by
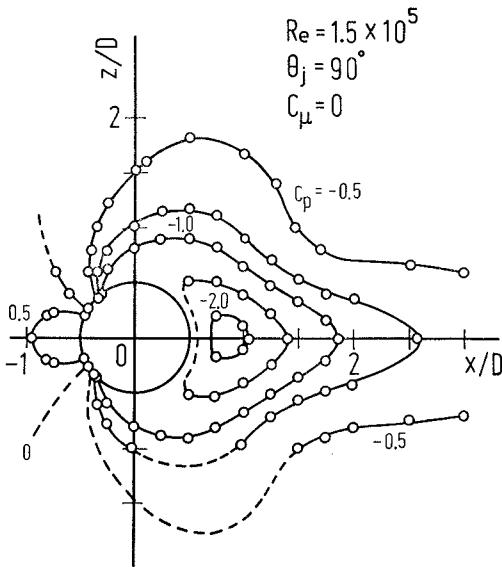

Fig.4 Pressure distribution on the side-wall
when $C_\mu = 0$.

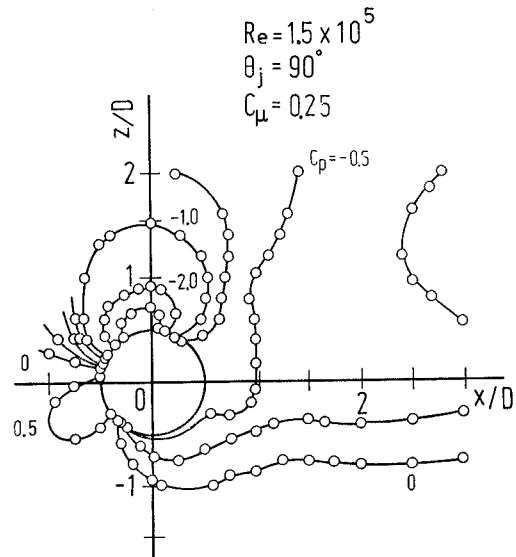
Fig.5 Pressure distribution on the side-wall
when $C_\mu = 0.25$.

proportional distribution among measured values at the nearby positions illustrated in Fig. 3. The solid lines are those obtained by smoothly connecting the symbols. The values on the cylinder surface are replaced by those at the distance of 3 mm from the juncture.

When $C_\mu = 0$, the pressure distribution seems to be symmetrical with respect to x-axis. The lowest pressure region exists right behind the cylinder, i.e., at x/D $\fallingdotseq$ 0.8 and the pressure gradually increases downstream. This pressure distribution is qualitatively equal to that at the mid-span.[3] It is naturally thought that this pressure distribution induces the secondary flow on the side-wall. The adverse pressure gradient downstream the cylinder on x-axis may cause the reverse flow toward the cylinder, which results in the formation of a pair of vortices.[1],[2]

When $C_\mu > 0$, the pressure distribution is no longer symmetrical with respect to x-axis. In general, the pressure on the upper-half of the side-wall becomes lower and that on the lower-half becomes higher than those of the corresponding sides in the case of $C_\mu = 0$, respectively. This pressure distribution also resembles that in the mid-span[3]. The lowest pressure region moves from the rear part toward the shoulder of the cylinder and the pressure drop there, which seems to be caused also by suction effect of the blowing jet, is in particular remarkable. Therefore it is thought that the change of the pressure distribution on the side-wall changes the pattern of the secondary flow.

The lower pressure on the upper-half of the side-wall than on the lower-half will induce the upward secondary flow, namely the upwash near the juncture, which will cause a pair of vortices to move upward. The stronger pressure drop near the shoulder may induce the stronger upper vortex of a pair of vortices in the place nearer to the cylinder while the almost invisible adverse pressure gradient will reduce the strength of the lower vortex of them in the place farther downstream. These are corresponding with the behavior of a pair of vortices formed behind the cylinder on the side-wall[1],[2]. Namely the upper one of a pair of vortices moves counterclockwise with increasing its strength and the lower one moves clockwise with decreasing its strength as C_μ increases. After all the lower vortex disappears and the upper one only remains when C_μ is extremely strong as already mentioned in detail[1],[3].

Figs. 6 and 7 show the pressure distributions on the side-wall when the values of θ_j and C_μ are properly adjusted under constant R_e so as to obtain nearly the same lift coefficients with each other at the mid-span. It is seen from these figures that it is not the mere inference that if the lift coefficients at the mid-span are equal to each other, the pressure must be distributed much the same way on the side-wall independently of θ_j and C_μ. This result is very interesting and seems to be connected with the similarity of the flow[6] near the juncture in this case.
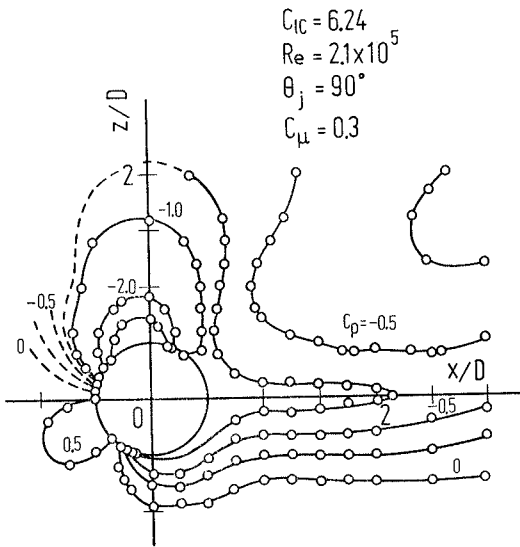
$$C_{lC} = 6.24$$
$$Re = 2.1 \times 10^5$$
$$\theta_j = 90°$$
$$C_\mu = 0.3$$

**Fig. 6 Pressure distribution on the side–wall
when C_{lc} = 6.24.**

$$C_{lC} = 6.35$$
$$Re = 2.1 \times 10^5$$
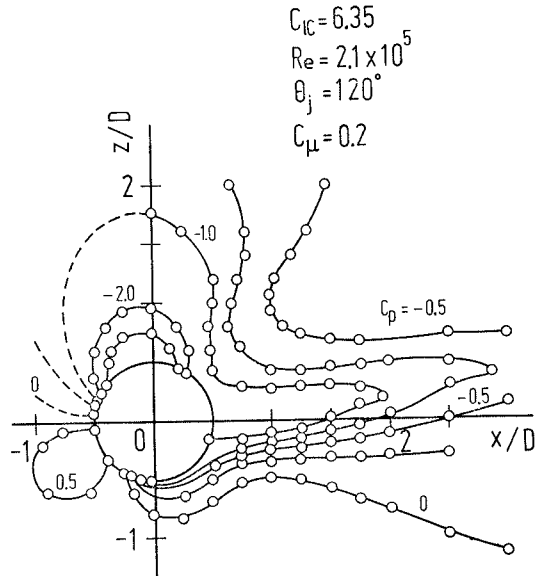$$\theta_j = 120°$$
$$C_\mu = 0.2$$

**Fig. 7 Pressure distribution on the side–wall
when C_{lc} = 6.35.**

The pressure distribution on the cylinder near the starboard side-wall is shown in Fig. 8. The upper and lower separation lines move upstream and downstream as the side-wall is approached, respectively. It is thought that this movement of the separation lines near the side-wall has a dominant effect on three dimensionality of the wake.

The lowest pressure point in the separated region lies on the upper side near the side-wall, that is, $y_w/D \doteq 0.6$ and $\theta \doteq 170°$. This point seems to be at the position of the center of the vortex shed directly from the cylinder surface since that position is corresponding to the central position (core) of the trailing vortex visualized with the dye-injection method and the tuft method[1),3)]. The secondary flow toward the lowest pressure point in the separated region ought to be induced counterclockwise due to the

$$Re = 2.1 \times 10^5 \quad \theta_j = 90° \quad C_\mu = 0.3$$
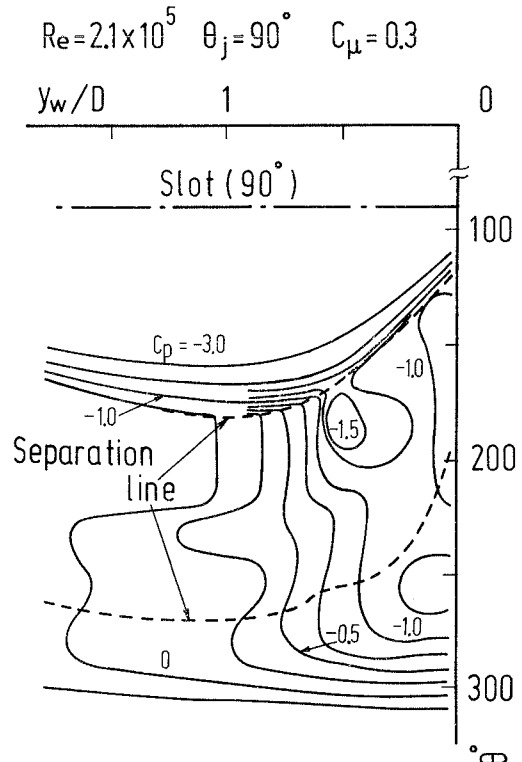
**Fig. 8 Pressure distribution on tne cylinder
near the starboard side-wall.**

downwash on the left side of that point and the upwash on the right side, and
entrained into the core of the vortex (the lowest pressure region) mentioned above.
The secondary flow near the cylinder-side-wall juncture becomes stronger with
increase of C_μ, since this three dimensionality of the pressure distribution near the
juncture is strengthened with increase of C_μ.

5 Concluding remarks

The pressure distributions on the surfaces of the cylinder and the side-wall were
measured to confirm the flow pattern already visualized by means of several tech-
niques. Consequently it is found that the results obtained in this investigation are
consistent with the visualized flow pattern and vortex system near the juncture, and
the results of the other investigations[1]~[6].

References

1) Yoshino, Waka and Hayashi, 6th Symposium on Flow Visualization, (1978-7), 43.
2) Yoshino and others, Preprint of Bulletin of JSME, No. 775-2 (1977-10), 136.
3) Yoshino and Waka, Reports of the Faculty of Engineering, Tottori University, 6-1 (1976-3), 1.
4) Furuya, Yoshino and Waka, Preprint of Bulletin of JSME and JSPE, (1974-11), 7.
5) Yoshino and others, Preprint of Bulletin of JSME, No. 775-2 (1977-10), 133.
6) Yoshino and others, Preprint of Bulletin of JSME, No. 808-2 (1980-5), 140.